Development of a Time of Flight Spectrometer for Application to Neutron Depth Profiling

S. M. Centiner,[1,2] K. Ünlü,[1,2] R. G. Downing,[3] M. Gordon[4]

Service Provided: Neutron Beam Laboratory

Introduction

Neutron depth profiling (NDP) is a near-surface analysis technique to measure the spatial distribution of certain light isotopes of technological importance in substrates with low neutron affinity. Ziegler [1,2] first reported the use of neutron depth profiling as a nuclear reaction analysis (NRA) technique to obtain boron profiles in semiconductors. Biersack et al [3] later thoroughly investigated and improved the technique to almost present capabilities.

Upon neutron absorption, certain light isotopes emit a charged particle, either a proton or alpha depending on the isotope, and a recoil nucleus. The particle emission is monoenergetic and isotropic. As the charged particle and the recoil move in the substrate they lose kinetic energy through nuclear and coulombic interactions with host atoms. The amount of energy loss can then be correlated to the distance traveled by the particles, which is an indication of the depth at which the particles are created.

Conventionally, neutron depth profiling is based on the direct measurement of particle energies by charged particle detectors, mostly by silicon semiconductor detectors. This technique is called conventional because almost all of the NDP measurements to date have been done through direct measurements of particle energies. Charged particle semiconductor detectors can be one of surface barrier detectors (SBD), passivated implanted planar silicon (PIPS) detectors or PIN photodiodes.

Neutron depth profiling has been used extensively for obtaining the depth profile of light elements in various fields. However, proportional to the advances in scientific and technological applications, depth profiling with higher resolutions has become a necessity. It can be shown that neutron depth profiling has reached the limits of resolution that can be attained by the conventional techniques. Time-of-flight neutron depth profiling (TOF-NDP) is proposed as an alternative approach to overcome the restraints that keep the conventional technique from achieving a higher resolution.

Parallel Electric Magnetic (PEM) Field Spectrometer

In the PEM field spectrometer, the nominal electron velocity is parallel to the direction of both the electric and magnetic fields. The electron accelerates as it approaches the detector because of the electrostatic force exerted on it. However, the net magnetomotive force is zero for an electron moving in the direction of the magnetic field.

A three-dimensional drawing of the spectrometer is shown in Figure 1. The ion beam enters through a $5\text{-}mm$ aperture on a tantalum disk at an angle of $15°$. The first disk has the carbon foil on a $3\text{-}mm$ aperture. The ion beam continues on its path with insignificant distortion in its direction. However, it loses a portion of its kinetic energy as it passes the foil, which must be taken into account in obtaining the energy spectra. The beam is extracted on the exit side of the stages through the apertures, where it is finally detected by the ion microchannel plate. The electrons generated by the ion emerge from the carbon foil and attracted by acceleration stages. At each stage, the electron gains equal kinetic energy. The surface potential of the electron microchannel plate was adjusted so that the
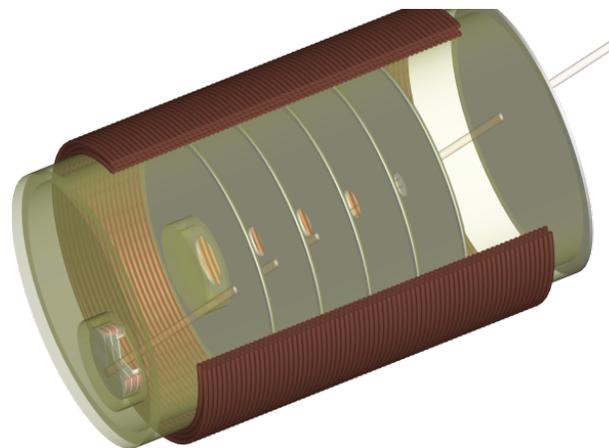
FIGURE 1: Three-dimensional drawing of the PEM field spectrometer

[1] Radiation Science and Engineering Center, Pennsylvania State University, University Park, PA 16802
[2] Department of Mechanical and Nuclear Engineering, Pennsylvania State University, University Park, PA 16802
[3] National Institute of Standards and Technology, Gaithersburg, MD 20899
[4] IBM T. J. Watson Research Center
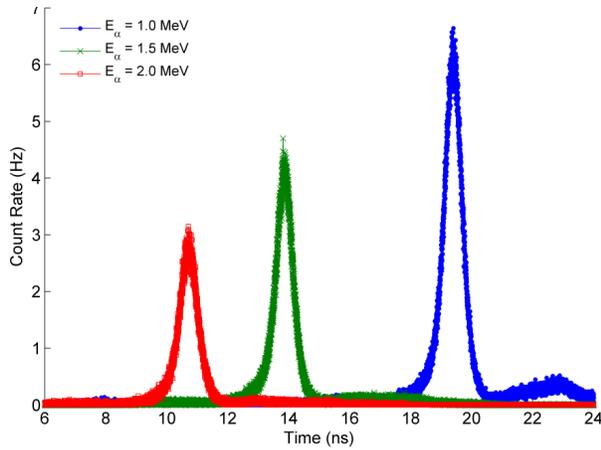
FIGURE 2: Time spectra obtained with 1.0, 1.5 and 2.0-MeV alpha beams
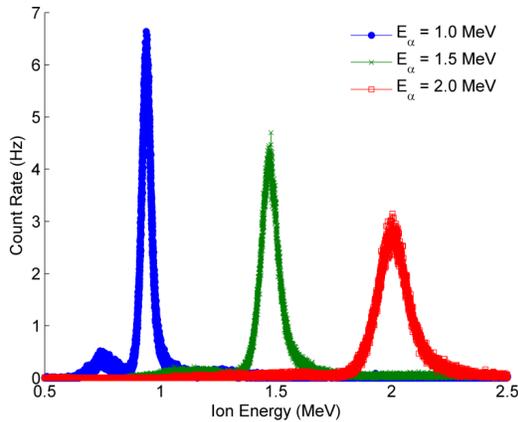
FIGURE 3: Energy spectra obtained from the offset and delay corrected time spectra
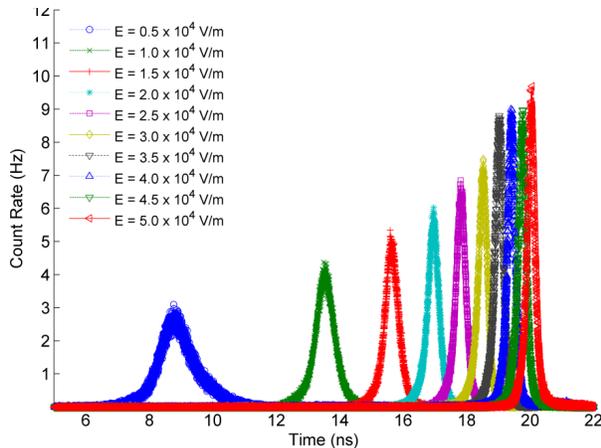
FIGURE 4: Time spectra of 1.5-MeV alpha beam at various electron acceleration fields

electric field between the exit plate and the micro-channel plate surface equals the electric field across the stages.

Response of the Spectrometer to Beam Energy

Time-of-flight spectra were taken with 1.0, 1.5 and 2.0-MeV alpha beams. In these measurements, the electron detector signal was used as the start trigger and the ion detector signal as the stop trigger. The carbon foil used as the secondary electron generator was 202-nm thick. The acceleration potential was set to $1000\ V$, which produced an electric field of $10^4\ V/m$. The magnetic field value required to map the electron beam with unity magnification was calculated $35 \times 10^{-4}\ T$, which corresponds to a solenoid current of $0.5\ A$. The time-of-flight spectra are shown in Figure 2. Since the signal from the electron microchannel plate was used as the starttrigger, the spectrum shifts left as the ion energy increases.

The standard deviations of the peaks were calculated as $266.6\ ps$, $253.5\ ps$, and $267.1\ ps$, respectively for 1.0, 1.5 and 2.0-MeV alpha beams. The energy spectra can be obtained from the offset and delay corrected time-of-flight spectra. Figure 3 shows the energy spectra of the alpha beams at 1.0, 1.5, and 2.0-MeV energy.

Response of the Spectrometer to Electron Accelerating Potential

A set of measurements was made to observe the effect of electron acceleration on peak resolution. The alpha beam energy was set to $1.5\ MeV$. A 50-nm thick carbon foil was used. The acquired spectra are plotted in Figure 4. The accelerating potential was varied from $500\ V$ to $5000\ V$ in $500\ V$ increments.

The improvement in peak resolution is conspicuous. The standard deviation of distributions start at approximately 420 ps for $500\ V$ and reduces to $110\ ps$ for $5000\ V$. The variation of the standard deviation is plotted in Figure 5. As can be seen in the figure, the spread drops off faster in the beginning, but it starts to level off as the electric field further increases. The limit it reaches, i.e. $\sim 100\ ps$, indicates other broadening mechanisms.

Figure 6 shows the energy spectra of 1.5-MeV alpha beams taken at three different acceleration potentials. The spectra were obtained by conversion of the time spectra shown in Figure 4. The centroids of the peaks are calculated as $1.481\ MeV$, $1.486\ MeV$, and $1.485\ MeV$ for 1000-V, 3000-V and 5000-V acceleration potentials. The standard deviations of the peaks are $35.51\ keV$, $18.97\ keV$ and $14.82\ keV$, respectively. The improvement in spectral resolution is significant as the acceleration potential is increased.

Cross Electric Magnetic (CEM) Field Spectrometer

A time-of-flight spectrometer was designed based on an earlier proposed design by Bowman et al [4]. An electric field is established between parallel frames at equal potential differences. The energetic ion goes
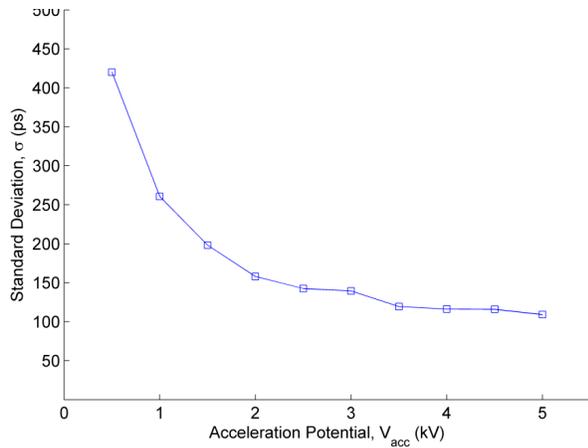
FIGURE 5: Improvement of the spectrometer resolution with the acceleration potential
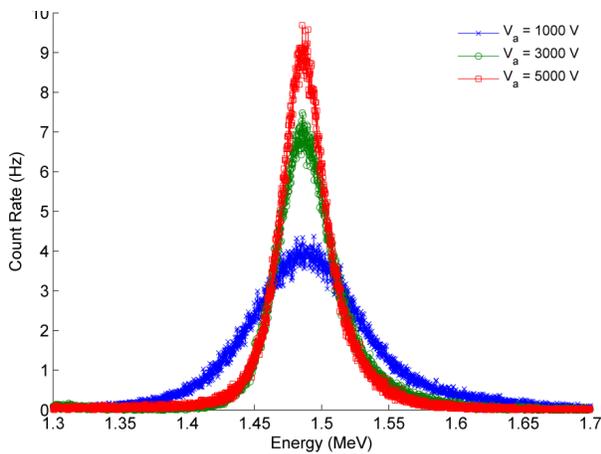
FIGURE 6: Energy spectra from corrected time spectra at different acceleration potentials

FIGURE 7: Electron acceleration unit of the CEM field spectrometer
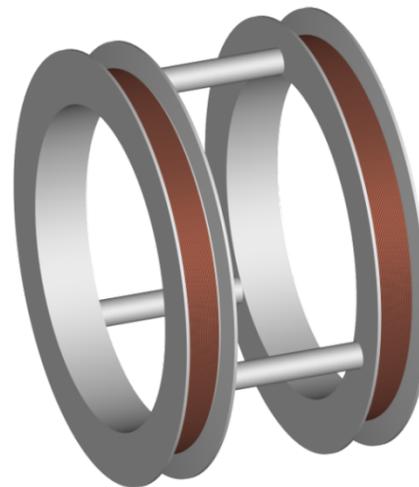
FIGURE 8: Helmholtz coil pair

through a thin carbon foil stretched on an aperture. The passage of the particle through the foil generates the secondary electrons. The ion continues on its straight path, exits the spectrometer and hits the ion detector. The generated electrons are focused on a microchannel plate positioned on the same plane with the carbon foil. A three-dimensional drawing of the electron acceleration unit is shown in Figure 7.

A Helmholtz pair consists of two identical circular magnetic coils that are placed symmetrically one on each side of the experimental area along a common axis, and separated by a distance equal to the radius of the coil. A cylindrical region extending between the centers of the two coils and approximately $1/5^{\text{th}}$ of the diameter will have a nearly spatially uniform magnetic field. The coil pair was constructed of $AWG\ \#23$ copper wire coated with regular enamel. The aluminum cores have an inner diameter of $150\ mm$. Each coil has $N = 725$ number of turns. The magnitude of maximum field at the center of the pair is

through each coil. A three-dimensional drawing of the Helmholtz coil is shown in Figure 8.

Time-of-flight spectra were obtained at $150\ V$ and $600\ V$ acceleration potentials. The magnet current was adjusted to create a magnetic field value that matches the electric field value to transport the ejected electrons onto the electron microchannel plate. In this measurement, the signal from the ion microchannel plate was used as the start trigger, and the electron signal was used as the stop trigger. The stop signal line was delayed by $\tau_{\text{delay}} = 60\ ns$. The data from the measurements is plotted in Figure 9.

The peak centroids were calculated to be at $13.264\ ns$ for $600\ V$ and $18.314\ ns$ for $150\ V$, from which the spectral shift was found $\Delta\tau_{\text{exp}} = 5.049\ ns$. Using the definition of cycloid period $\tau = {2\pi m_e}/{e_0 B}$, the expected spectral shift can be calculated as follows:
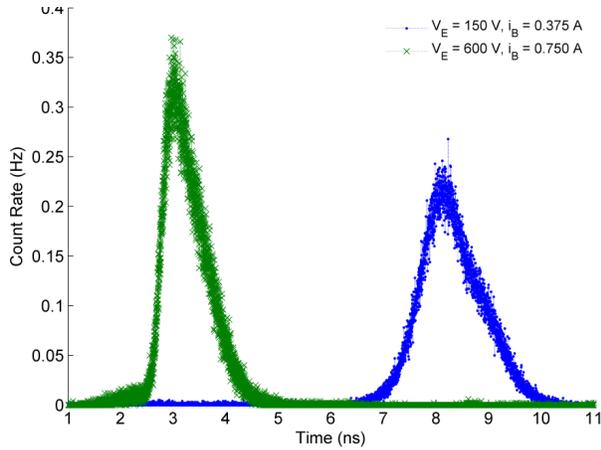
FIGURE 9: Time spectra obtained at two acceleration potentials
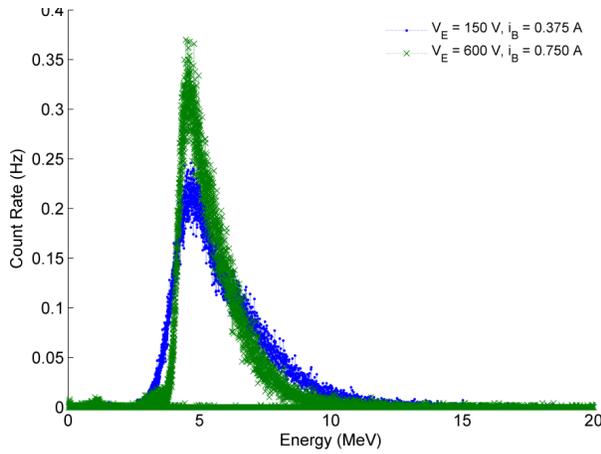
FIGURE 10: Energy spectra obtained by offset and delay corrected time spectra

$$\Delta\tau = \tau_2 - \tau_1 = \frac{2\pi m_e}{e_0}\left(\frac{1}{B_2} - \frac{1}{B_1}\right)$$

$$= \left(\frac{5}{4}\right)^{\frac{3}{2}} \frac{2\pi m_e r}{e_0 \mu_0 n}\left(\frac{1}{i_2} - \frac{1}{i_1}\right)$$

Using the parameters of the first designed Helmholtz coil, $r = 62.5\ mm, n = 600$, the expected shift from $i_1 = 0.375\ A$ to $i_2 = 0.750\ A$ is $\Delta\tau_{\text{theo}} = 4.993\ ns$, which is within 1% of the experimental result.

Figure 10 shows the energy spectra of the alphas ejected by the ^{210}Po source. The peak locations are found to be $4672\ keV$ for the spectrum acquired with $150\text{-}V$ acceleration, and $4631\ keV$ for the spectrum acquired with $600\text{-}V$ acceleration. From the TRIM simulation, the peak location was expected to be located at $4464\ keV$. The deviation between the measured and simulated results is within 5%. The major source of the deviation is the uncertainty in the thickness of the source layer: The manufacturer's specification gives a broad range for the thickness of the layer.

References

1. J. F. Ziegler, G. W. Cole, J. E. E. Baglin, J. Appl. Phys. **43**, 3809 (1972).
2. W. K. Chu, V. L. Moruzzi, J. F. Ziegler, J. Appl. Phys. **46**, 2817-2820 (1975).
3. J. P. Biersack, D. Fink, R. Henkelmann, K. Müller, Nuc. Inst. Meth. **149**, 93-97 (1978).
4. J. D. Bowman, R. H. Heffner, Nucl. Instrum. Meth. **148**, 503-509 (1978).

Publications

1. S. M. Cetiner, K. Ünlü, R. G. Downing, *"Development of time-of-flight neutron depth profiling at Penn State University"*, presented in 11th Int. Conf. on Modern Trends in Activation Analysis, University of Surrey, Gilford, UK, 2004; J. Radioanal. Nucl. Ch. **217**, 275-281 (2007).
2. S. M. Cetiner, K. Ünlü, R. G. Downing, *"Development and applications of time-of-flight neutron depth profiling"*, presented in 7th Methods and Applications of Radioanalytical Chemistry (MARC), Kona, HI, 2006; J. Radioanal. Nucl. Ch. **276**, 623-630 (2008).
3. S. M. Cetiner, K. Ünlü, *"Depth profiling of boron in ultra-shallow junction devices using time-of-flight neutron depth profiling (TOF-NDP)"*, presented in Symposium on Radiation Measurements and Applications, Ann Arbor, MI, 2006; Nucl. Instrum. Meth. Phys. Res. A **579**, 148-152 (2007).